

HNPS Advances in Nuclear Physics

Vol 27 (2019)

HNPS2019



Preliminary results on the study of $^{237}\text{Np}(n,f)$ at $n_TOF/EAR2$ in energies related to nuclear waste transmutation

Athanasios Stamatopoulos, and the n_TOF Collaboration

doi: [10.12681/hnps.2472](https://doi.org/10.12681/hnps.2472)

To cite this article:

Stamatopoulos, A., & the n_TOF Collaboration, and. (2020). Preliminary results on the study of $^{237}\text{Np}(n,f)$ at $n_TOF/EAR2$ in energies related to nuclear waste transmutation. *HNPS Advances in Nuclear Physics*, 27, 18–24. <https://doi.org/10.12681/hnps.2472>

Preliminary results on the study of $^{237}\text{Np}(n,f)$ at n_TOF/EAR2 in energies related to nuclear waste transmutation

A. Stamatopoulos¹, A. Tsinganis², M. Diakaki^{1,44}, N. Colonna³, M. Kokkoris¹, R. Vlastou¹, A. Kalamara¹, P. Schillebeeckx⁴, L. Tassan-Got⁵, P. Žugec^{6,2}, M. Sabaté-Gilarte^{2,7}, N. Patronis⁸, Z. Eleme⁸, J. Heyse⁴, O. Aberle², J. Andrzejewski⁹, L. Audouin⁵, M. Bacak^{10,2,11}, J. Balibrea¹², M. Barbagallo³, F. Bečvář¹³, E. Berthoumieux¹¹, J. Billowes¹⁴, D. Bosnar⁶, A. Brown¹⁵, M. Caamaño¹⁶, F. Calviño¹⁷, M. Calviani², D. Cano-Ott¹², R. Cardella², A. Casanovas¹⁷, F. Cerutti², Y. H. Chen⁵, E. Chiaveri^{2,14,7}, G. Cortés¹⁷, M. A. Cortés-Giraldo⁷, L. Cosentino¹⁸, L. A. Damone^{3,19}, C. Domingo-Pardo²⁰, R. Dressler²¹, E. Dupont¹¹, I. Durán¹⁶, B. Fernández-Domínguez¹⁶, A. Ferrari², P. Ferreira²², P. Finocchiaro¹⁸, V. Furman²³, K. Göbel²⁴, A. R. García¹², A. Gawlik⁹, S. Gilardoni², T. Glodariu⁴²⁵, I. F. Gonçalves²², E. González-Romero¹², E. Griesmayer¹⁰, C. Guerrero⁷, F. Gunsing^{9,12}, H. Harada²⁶, S. Heinitz²¹, D. G. Jenkins¹⁵, E. Jericha¹⁰, F. Käppeler²⁷, Y. Kadi², P. Kavargin¹⁰, A. Kimura²⁶, N. Kivel²¹, I. Knapova¹³, M. Krtička¹³, D. Kurtulgil²⁴, E. Leal-Cidoncha¹⁶, C. Lederer²⁸, H. Leeb¹⁰, J. Lerendegui-Marco⁷, S. Lo Meo^{29,30}, S. J. Lonsdale³³, D. Macina², A. Manna^{30,31}, J. Marganec^{9,32}, T. Martínez¹², A. Masi², C. Massimi^{30,31}, P. Mastinu³³, M. Mastromarco³, E. A. Mauger²¹, A. Mazzone^{3,34}, E. Mendoza¹², A. Mengoni²⁹, P. M. Milazzo³⁵, F. Mingrone², A. Musumarra^{18,36}, A. Negret²⁵, R. Nolte³², A. Oprea²⁵, A. Pavlik³⁷, J. Perkowski⁹, I. Porras³⁸, J. Praena³⁸, J. M. Quesada⁷, D. Radeck³², T. Rauscher^{39,40}, R. Reifarth²⁴, C. Rubbia², J. A. Ryan¹⁴, A. Saxena⁴¹, D. Schumann²¹, P. Sedyshev²³, A. G. Smith¹⁴, N. V. Sosnin¹⁴, G. Tagliente³, J. L. Tain²⁰, A. Tarifeño-Saldivia¹⁷, S. Valenta¹³, G. Vannini^{30,31}, V. Variale³, P. Vaz²², A. Ventura³⁰, D. Vescovi^{3,42}, V. Vlachoudis², A. Wallner⁴³, S. Warren¹⁴, C. Weiss¹⁰, P. J. Woods²⁸, and T. Wright¹⁴ and the n_TOF Collaboration

¹ National Technical University of Athens, Greece

² European Organization for Nuclear Research (CERN), Switzerland

³ Istituto Nazionale di Fisica Nucleare, Sezione di Bari, Italy

⁴ European Commission, Joint Research Centre, Geel, Retieseweg 111, B-2440 Geel, Belgium

⁵ Institut de Physique Nucléaire, CNRS-IN2P3, Univ. Paris-Sud, Université Paris-Saclay, F-91406 Orsay Cedex, France

⁶ Department of Physics, Faculty of Science, University of Zagreb, Zagreb, Croatia

⁷ Universidad de Sevilla, Spain

⁸ University of Ioannina, Greece

⁹ University of Lodz, Poland

¹⁰ Technische Universität Wien, Austria

¹¹ CEA Irfu, Université Paris-Saclay, F-91191 Gif-sur-Yvette, France

¹² Centro de Investigaciones Energéticas Medioambientales y Tecnológicas (CIEMAT), Spain

¹³ Charles University, Prague, Czech Republic

¹⁴ University of Manchester, United Kingdom

¹⁵ University of York, United Kingdom

¹⁶ University of Santiago de Compostela, Spain

¹⁷ Universitat Politècnica de Catalunya, Spain

¹⁸ INFN Laboratori Nazionali del Sud, Catania, Italy

¹⁹ Dipartimento di Fisica, Università degli Studi di Bari, Italy

²⁰ Instituto de Física Corpuscular, CSIC - Universidad de Valencia, Spain

²¹ Paul Scherrer Institut (PSI), Villingen, Switzerland

²² Instituto Superior Técnico, Lisbon, Portugal

²³ Joint Institute for Nuclear Research (JINR), Dubna, Russia

²⁴ Goethe University Frankfurt, Germany

²⁵ Horia Hulubei National Institute of Physics and Nuclear Engineering, Romania

²⁶ Japan Atomic Energy Agency (JAEA), Tokai-mura, Japan

²⁷ Karlsruhe Institute of Technology, Campus North, IKP, 76021 Karlsruhe, Germany

²⁸ School of Physics and Astronomy, University of Edinburgh, United Kingdom

²⁹ Agenzia nazionale per le nuove tecnologie (ENEA), Bologna, Italy

- ³⁰ *Istituto Nazionale di Fisica Nucleare, Sezione di Bologna, Italy*
³¹ *Dipartimento di Fisica e Astronomia, Università di Bologna, Italy*
³² *Physikalisch-Technische Bundesanstalt (PTB), Bundesallee 100, 38116 Braunschweig, Germany*
³³ *Istituto Nazionale di Fisica Nucleare, Sezione di Legnaro, Italy*
³⁴ *Consiglio Nazionale delle Ricerche, Bari, Italy*
³⁵ *Istituto Nazionale di Fisica Nucleare, Sezione di Trieste, Italy*
³⁶ *Dipartimento di Fisica e Astronomia, Università di Catania, Italy*
³⁷ *University of Vienna, Faculty of Physics, Vienna, Austria*
³⁸ *University of Granada, Spain*
³⁹ *Department of Physics, University of Basel, Switzerland*
⁴⁰ *Centre for Astrophysics Research, University of Hertfordshire, United Kingdom*
⁴¹ *Bhabha Atomic Research Centre (BARC), India*
⁴² *Istituto Nazionale di Fisica Nucleare, Sezione di Perugia, Italy*
⁴³ *Australian National University, Canberra, Australia*
⁴⁴ *CEA, Cadarache, DEN/DER/SPRC/LEPh, 13108 Saint Paul Les Durance, France*

Abstract The accurate knowledge of neutron-induced fission cross sections of isotopes involved in the nuclear fuel cycle is essential for the optimum design and safe operation of next generation nuclear systems. Such experimental data can additionally provide constraints for the adjustment of nuclear model parameters used in the evaluation process, resulting in a further understanding of the nuclear fission process. In this respect measurements of the $^{237}\text{Np}(n,f)$ cross section have been performed at the n_{TOF} facility at CERN in the horizontal 185 m flight-path (EAR1) which were discrepant by 7% in the MeV region. The neutron-induced fission cross section of $^{237}\text{Np}(n,f)$ was recently restudied at the EAR2 19.5 m vertical beam-line at CERN's n_{TOF} facility, over a wide range of neutron energies, from 100 keV up to 15 MeV, using the time-of-flight technique and a modern set-up based on Micromegas detectors. This study was performed in an attempt to resolve the aforementioned discrepancies and to provide accurate data of a reaction that is frequently used as reference in measurements related to feasibility and design studies of advanced nuclear systems. Preliminary results with a high statistical accuracy that resolve the discrepancies will be presented along with a brief discussion concerning the facility and the analysis.

Keywords neutron-induced fission, cross section, time of flight, n_{TOF} EAR2, nuclear waste

Corresponding author: A. Stamatopoulos (athanasios.stamatopoulos@cern.ch) | Published online: May 1st, 2020

INTRODUCTION

The neutron-induced fission cross section of ^{237}Np is frequently used as a reference reaction in measurements due to its low fission threshold in addition to the fact that neptunium samples, suitable for fission, feature a moderate activity. Due to this particular usage, this reaction is included in the High Priority Request List [1] with 2–3% target accuracy in the 200 keV – 20 MeV energy region [2]. In addition, a monitoring scheme was approved by the IAEA to keep track of separated ^{237}Np since it can be potentially used in nuclear explosive devices [3]. In this regard, neptunium can be used as a nuclear fuel in fast reactors thus achieving the minimisation of its proliferation, which additionally justifies the importance of the $^{237}\text{Np}(n,f)$ cross section. In this respect a plethora of measurements have been reported in the EXFOR database [4] since the late 40's, three of which were performed the last decade at n_{TOF} (Paradela et al. [5], Diakaki et al. [6]) and at NCSR “Demokritos” (Diakaki et al. [7]) and were found to be 7% discrepant in the energy region between 1 and 5 MeV. To resolve these discrepancies, the $^{237}\text{Np}(n,f)$ reaction was studied at CERN's n_{TOF} facility at the 19.5 m vertical flight path referred to as EAR2, covering a large portion of the HPRL request up to 14 MeV.

EXPERIMENTAL DETAILS

The n_TOF/EAR2 facility at CERN

The study of the $^{237}\text{Np}(n,f)$ reaction took place at the n_TOF facility at CERN. More specifically, the 19.5 m vertical flight path, commonly referred to as EAR2 [8] was used which delivers a high instantaneous neutron flux that spans from the meV to the MeV region, as shown in fig. 1. This wide neutron spectrum was produced by spallation reactions induced by a 20 GeV/c pulsed proton beam, delivered by CERN's PS accelerator, that impinged on a 40 cm in length and 60 cm in diameter lead block. The wide spectrum seen in fig. 1 is a result of the neutron moderation inside the water layer that surrounds the spallation target.

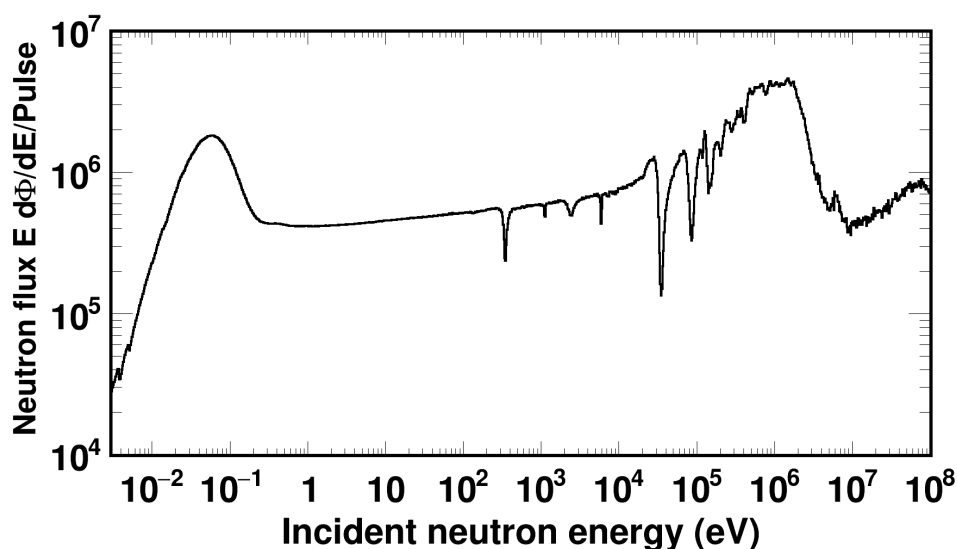


Figure 1. The neutron flux provided at EAR2 spans across a broad energy range covering more than 10 orders of magnitude.

The time of flight technique

The incident neutron energy is calculated through the time difference between the neutron production and its arrival in the detector. The former time can be estimated from the spallation γ -rays that arrive in the experimental hall, while the latter is the time that the fission signal was formed. This time difference is then converted to energy, using the flight path $L = 19.5$ m and the non-relativist formula.

The fission foils

Four neptunium samples were prepared at EC-JRC-Geel using the molecular plating technique on bulk neptunium dioxide material. The total ^{237}Np mass was 1.8 mg, the diameter of each foil was 3 cm thus yielding an average $60 \mu\text{g}/\text{cm}^2$ average areal density.

An additional neptunium foil was provided by IPN-Orsay, which was produced by electrodeposition and had a 1.48 mg mass and a 3 cm diameter. The purpose of this additional sample was to study possible systematic effects in the reaction yield calculation, that might be attributed to the different batch material or the preparation process.

Finally, two ^{238}U and a ^{235}U samples were used as reference foils. The diameter of the samples still remained 3 cm while the total mass was 3.76 mg and 0.51 mg for ^{238}U and ^{235}U , respectively.

The detectors

To detect the fission fragments, an assembly based on the compact and high-gain gaseous Micromegas detectors was used [9]. The Micromegas detector consists of two main regions : (a) *The drift volume* (5mm) in which fission fragments ionise the gas, producing electrons which then drift towards (b) *the amplification region* (50 μm) where an avalanche multiplication takes place. A schematic representation of the Micromegas detector can be seen in fig. 2.

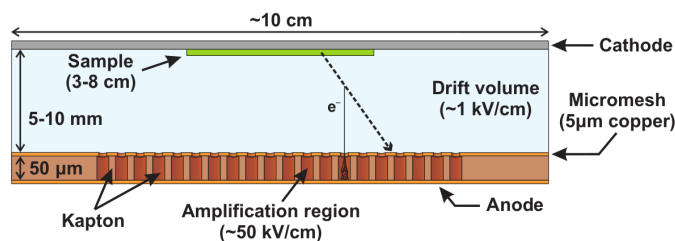


Figure 2. A schematic representation of a Micromegas detector used in n_{TOF} fission studies.

The two regions are separated by a thin (5 μm) conductive electrode which is covered in holes, as seen in fig. 3. The holes allow the gas flow and primary electron transport between the drift and amplification region. The distance between the holes, commonly referred to as pitch, is of the order of 50 μm while the diameter is of the order of 65 μm .

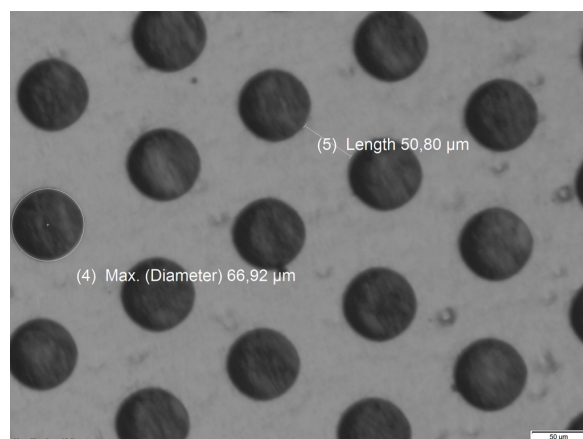


Figure 3. Optical microscope image of the micromesh. The dark circular regions correspond to the micromesh holes. The typical distance between holes and its diameter are also visible.

The detectors along with the fission foils were housed in a cylindrical aluminium chamber which was filled with $\text{Ar}:\text{CF}_4:\text{iC}_4\text{H}_{10}$ at 88:10:2 volume fraction and atmospheric pressure and temperature.

The n_{TOF} data acquisition system

Data at n_{TOF} consisted of digitized waveforms that were recorded by 14-bit flash analogue-to-digital converters at a 225 MHz sampling rate. The data are then transferred on tape and were stored for subsequent offline analysis.

DATA REDUCTION AND ANALYSIS

Raw data are processed offline by a set of pulse processing routines [10]. The signal identification was based on a differentiation filter and for each detector signal a set of attributes is

extracted such as its tof, amplitude, area, FWHM etc. To ensure an efficient estimation of the aforementioned attributes pulse shape analysis was applied. That information is finally stored in so-called list mode and finally the reaction yield Y was calculated based on eq. (1).

$$Y = \frac{C f_{amp} f_{DT} f_{\gamma f} f_{shield} f_{SF}}{\Phi} \quad (1)$$

where :

1. C are the recorded fission events
2. f_{amp} is the correction due to the amplitude cut that was applied to reject α -particle events from the decay of the samples
3. f_{DT} is the dead time correction factor
4. $f_{\gamma f}$ is the correction due to photo-fission events
5. f_{SF} is the correction due to spontaneous fission
6. Φ is the incident neutron flux

The determination of f_{amp} was based on Monte Carlo simulations by coupling the GEF [11] and FLUKA [12] codes. Fission fragments distribution from GEF, were generated within the volume of the fission foil and fragments were then propagated towards the gas in order to estimate the energy deposition. The energy deposition was then calibrated to match the pulse height spectrum and thus estimate the low amplitude tails and consequently the fraction of rejected fission fragments, as illustrated in fig. 4 (shaded area) for an amplitude cut of 300 channels. The simulations were performed for each individual fission foil and correction factors of the order of 5-6% were estimated.

Concerning the dead-time correction the methodology that was used, is described in detail in [13]. In the present case correction factors of the order of a few percent were estimated for the EC-JRC samples and less than 40% for the IPN-Orsay one.

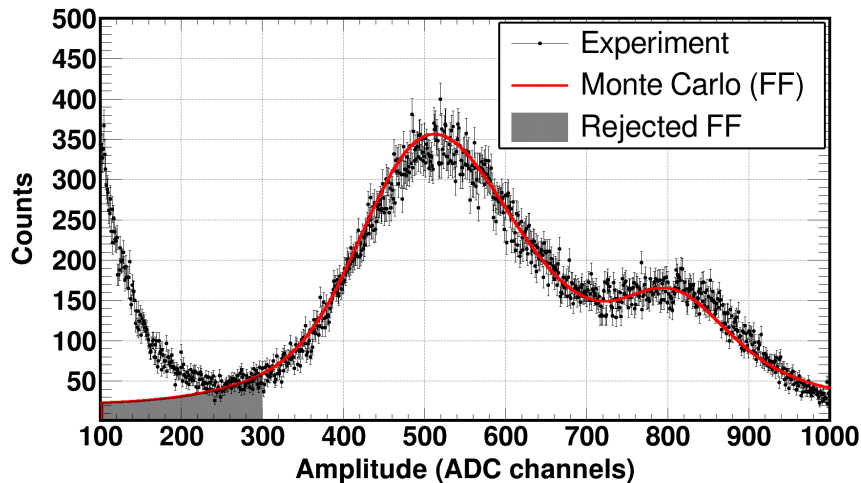


Figure 4. Experimental pulse height spectra (black points) and simulated energy deposition of fission fragments (red solid curve). The shaded area corresponds to the rejected fission fragment (FF) events due to the application of a 300 channels amplitude threshold

The contribution of photo-fission events to the recorded fission yield was estimated through the use of Monte Carlo simulations that were available from the n_TOF collaboration. More specifically, the time and energy distribution of photons that were produced from spallation reactions and reached the experimental area was estimated at the level of each fission foil. The ENDF/B-VIII.0 (γ, f) cross sections were then used to estimate the photo-fission reaction rate which was then compared to the experimental one, in the time-of-flight domain. As shown in fig. 5, a less than 0.1% contribution was

estimated, thus the recorded fission events were considered to be attributed only to neutron-induced fission.

Finally, spontaneous fission events experimentally estimated from beam-off runs and their contribution was negligible.

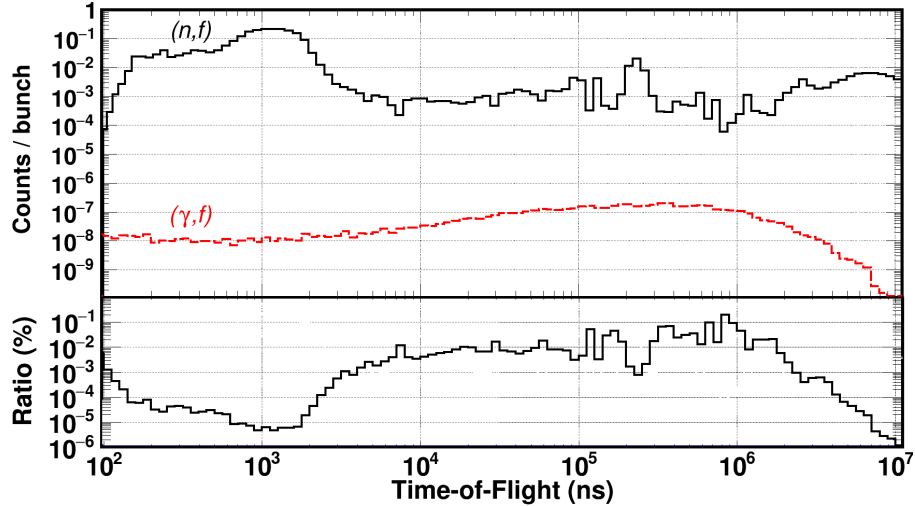


Figure 5. Top panel: Simulated photo-fission events (red dashed curve) in comparison with experimental counts (black solid curve). Bottom panel: The contribution of photon-induced fission events did not exceed 0.1 %, therefore considered negligible.

The cross section (σ) was then calculated with reference to the $^{235}\text{U}(n,f)$ one (σ_{ref}), using eq. (2)

$$\sigma = \frac{Y}{Y_{ref}} \frac{N_{ref}}{N} \sigma_{ref} \quad (2)$$

where N corresponds to the number of nuclei in the fission foils and the subscript “ref” refers to the reference sample. Since the beam delivered at n_TOF was parallel, the incident neutron flux Φ to the fission foils was the same, therefore was not considered in the calculation.

RESULTS AND DISCUSSION

The preliminary $^{237}\text{Np}(n,f)$ neutron-induced cross section was calculated from two fission foils with reference to the $^{235}\text{U}(n,f)$ one in the energy range between 200 keV – 14 MeV, as shown in fig. 6, in comparison to the data reported by Diakaki et al. [6] and Paradela et al. [5]. The present data, although preliminary, confirm the data reported by Diakaki et al. [6], thus providing additional constraints in future evaluations.

CONCLUSIONS

The $^{237}\text{Np}(n,f)$ cross section was studied at the EAR2 beam-line at the n_TOF facility at CERN using Micromegas detectors. Data were recorded from 9 meV up to 14 MeV covering a broad neutron energy range. Preliminary data were analyzed between 200 keV and 14 MeV, covering a large portion of the IAEA requirements. The preliminary cross section was in agreement with the data by Diakaki et al. [6], thus resolving the discrepancies that were observed in recent measurements. The analysis is expected to be completed in the near future.

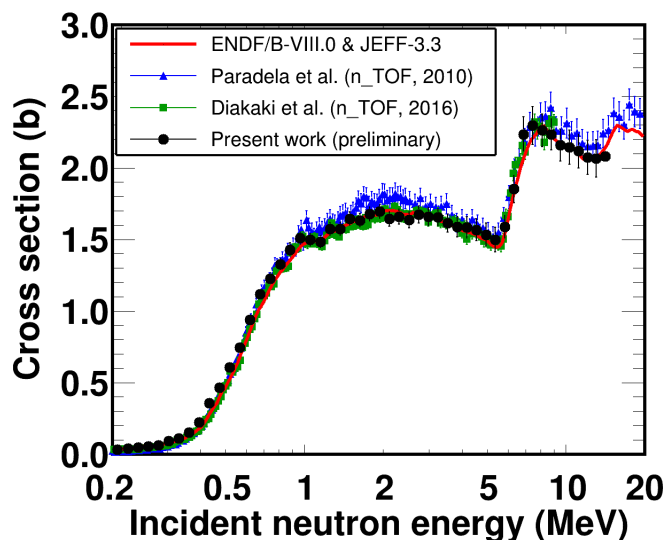


Figure 6. The preliminary $^{237}\text{Np}(n,f)$ cross section reported in the present work in the 200 keV – 14 MeV energy range, is in agreement with the cross section reported by Diakaki et al. [6].

Acknowledgments

This research is implemented through IKY scholarships program and co-financed by the European Union (European Social Fund —ESF) and Greek national funds through the action entitled “Reinforcement of Postdoctoral Researchers - 2nd call (MIS 5033021)”, in the framework of the Operational Programme “Human Resources Development Program, Education and Lifelong Learning” of the National Strategic Reference Framework

References

- [1] The High Priority Request List (HPRL), <https://www.oecd-neo.org/dbdata/hprl/>
- [2] High priority request ID 44 : $^{237}\text{Np}(n,f)$, <https://www.oecd-neo.org/dbdata/hprl/hprlview.pl?ID=464>
- [3] Tech. Rep., IAEA (2016), https://www-pub.iaea.org/MTCD/Publications/PDF/SVS_33_web.pdf
- [4] N. Otuka et. al., Nucl. Data Sheets 120, 272 (2014)
- [5] C. Paradela, for the n_TOF Collaboration, Phys. Rev. C 82, 034601 (2010)
- [6] M. Diakaki et al., Eur. Phys. J. A 49, 62 (2013)
- [7] M. Diakaki et al., Nucl. Data Sheets 119, 52 (2014)
- [8] C. Weiss et al., Nucl. Instrum. Meth. A 799, 90 (2015)
- [9] S. Andriamonje et. al., J. Kor. Phys. Soc. 59, 1601 (2011)
- [10] P. Žugec et al., Nucl. Instrum. Meth. A 812, 134 (2016)
- [11] K.-H. Schmidt et al., Tech. Rep. NEA/DB/DOC(2014)1, OECD (2014)
- [12] A. Ferrari et al., Tech. Rep., CERN-2005-10 (2005)
- [13] A. Stamatopoulos et al., Nucl. Instrum. Meth A 913, 40 (2019)